Available online at www.sciencedirect.com
SCIENCE DIRECT
Scripta Materialia 55 (2006) 335–338
Scripta MATERIALIA
www.actamat-journals.com

Failure of brittle layers on polymeric substrates from Vickers indentation

Herzl Chai[a] and Brian R. Lawn[b,*]

[a] *Department of Solid Mechanics, Materials and Systems, Tel Aviv University, Tel Aviv, Israel*
[b] *Materials Science and Engineering Laboratory, National Institute of Standards and Technology, Gaithersburg, MD 20899-8500, USA*

Received 16 December 2005; revised 13 April 2006; accepted 27 April 2006
Available online 23 May 2006

A study is made of median crack evolution in brittle coatings subjected to sharp contacts. A model bilayer system consisting of a glass plate bonded to a polycarbonate base, with a Vickers pyramid as indenter, is used to demonstrate the evolution in situ. The cracks undergo a phase of stable downward growth with increasing load. Beyond the coating mid-plane, flexural stresses (coupled with the local contact field) elongate and accelerate the median cracks through the plate to failure. Critical loads corresponding to this failure state diminish with decreasing layer thickness until, at small thicknesses, failure occurs spontaneously at initiation. Published by Elsevier Ltd. on behalf of Acta Materialia Inc.

Keywords: Vickers indentation; Median cracks; Brittle coatings; Glass; Bilayers

There are many examples of engineering and biomechanical bilayer systems consisting of hard and stiff coatings or films on compliant substrates—laminated windows, brittle coatings and films, teeth and dental crowns, and shells [1–8]. Hard and stiff protective layers offer effective stress shielding to an otherwise vulnerable underlayer. But such layers also tend to be brittle and therefore highly susceptible to fracture in concentrated loading, especially to sharp contacts. Recently, there has been a focus on the fracture of brittle layer systems in blunt (Hertzian) contacts, in simulation of occlusal contacts on dental crowns [9–13]. The two most prominent fracture modes in such fields are cone and median cracks [14]. Median cracks can be especially dangerous as the indenter radius diminishes, because they can initiate at small loads [15]. In contacts with a Vickers diamond pyramid, such cracks become totally dominant, and lead to the well-documented radial cracks that appear on the indented surfaces of flat monolithic ceramics [14,16]. Median cracks initiate at low loads from shear-driven microcrack-like flaws that generate within the "quasiplastic" hardness zone, and subsequently penetrate deep into the material as the load is increased [17–19]. Once median cracks enter the far field remote from the immediate indentation site the propagation becomes relatively independent of indenter radius and geometry [20]. In bilayers, flexure of the brittle coating can accelerate median cracks through the lower half of the plate, taking the system to premature failure [21].

In this communication we describe the evolution of median cracks in brittle layer coating systems beneath sharp indenters. Some limited data have been obtained previously for similar evolution using blunt indenters, where competition from preceding cone cracks tends to obscure the early stages of growth [20,22]. Here we use a Vickers indenter, in single-cycle loading, where median cracks constitute the sole fracture mode, from initiation to failure. Experiments are conducted on an optically transparent bilayer system—side-polished soda-lime glass plates on a polycarbonate base support—so that crack progress can be followed in situ during actual testing [12]. We pay particular attention to critical conditions to initiate the median cracks, and, especially, to drive these cracks through the plate to failure. Explicit if simplistic relations for defining the critical failure load in terms of basic variables, notably layer thickness and material toughness, are determined.

Model glass/polycarbonate bilayers were fabricated as described in previous studies [12]. Soda-lime glass plates of prescribed thicknesses $d = 100$ μm to 2.5 mm were bonded to polycarbonate bases 12.5 mm thick with a thin layer (≈20 μm) of epoxy adhesive. Most glass top and bottom surfaces were pre-etched to remove large surface flaws, so that the cracks could be guaranteed to initiate from the Vickers hardness zone. An exception

* Corresponding author. E-mail: brian.lawn@nist.gov

1359-6462/$ - see front matter Published by Elsevier Ltd. on behalf of Acta Materialia Inc.
doi:10.1016/j.scriptamat.2006.04.034

was made on a select few glass plates, in which the undersurfaces were abraded with grade 600 SiC grit to test the possibility of competing lower-surface radial cracks [12]. Side walls were polished to enable side viewing during testing.

The bonded bilayers were placed in a small test loading fixture mounted onto the stage of a transmission optical microscope, with the optical axis normal to the specimen side walls. A basic screw system was used to load the Vickers indenter, and a miniature load cell to measure the applied load. The indenter was oriented such that the impression diagonals were aligned parallel and perpendicular to the specimen sides. In this way the median crack length c below the indentation surface could be measured as a function of monotonically increasing Vickers load P for any given glass layer thickness d [23]. Load was applied continually such that failure occurred in ≈5 min.

A typical evolutionary sequence is shown in Figure 1, for a glass layer of thickness $d = 1.5$ mm. The photographs show only the upper portion of the glass plate. A median crack in the plane of the figure is visible as the subsurface-contained penny-like feature with interference fringes. (A second, edge-on median crack is visible along the contact axis.) The sequence is as follows: (a) generation of a hemispherical quasiplastic zone (dark shadow); (b) initiation of median cracks; (c) downward and outward extension of the median cracks; (d) continued extension (as in monolithic glass); (e) pronounced downward elongation of the median cracks as they approach the mid-section of the glass plate; (f) unstable penetration through the lower half of the plate thickness.

Figure 2 plots characteristic damage depth as a function of load for the case shown in Figure 1. It can be assumed that the quasiplastic zone contains incipient cracks of the same scale as the quasiplastic zone dimension a (unfilled symbols) [24]. At a threshold load $P \approx 40$ N, median cracks pop in to well-defined penny configurations of depth c (first arrow). Further increase in load drives these cracks steadily downward toward the lower portion of the plate (filled symbols). At load $P \approx 300$ N, the cracks penetrate unstably through the glass plate, to $c = d = 1.5$ mm (second arrow). Note that the functional dependencies $a(P)$ and $c(P)$ of the data are in accordance with the respective hardness (H) and toughness (K_c) relations for sharp indentations [25]

$$H = P/\alpha a^2 \tag{1a}$$

$$K_c = \chi P/c^{3/2} \tag{1b}$$

i.e. $a = (P/\alpha H)^{1/2}$ and $c = (\chi P/K_c)^{2/3}$, with $\alpha H = 12.4$ GPa and $K_c/\chi = 12.6$ MPa m$^{1/2}$ adjusted to give best fits. Eq. (1a) is based on the assumption of a size-invariant hardness, and Eq. (1b) on the assumption of a center-loaded penny crack. Although these relations

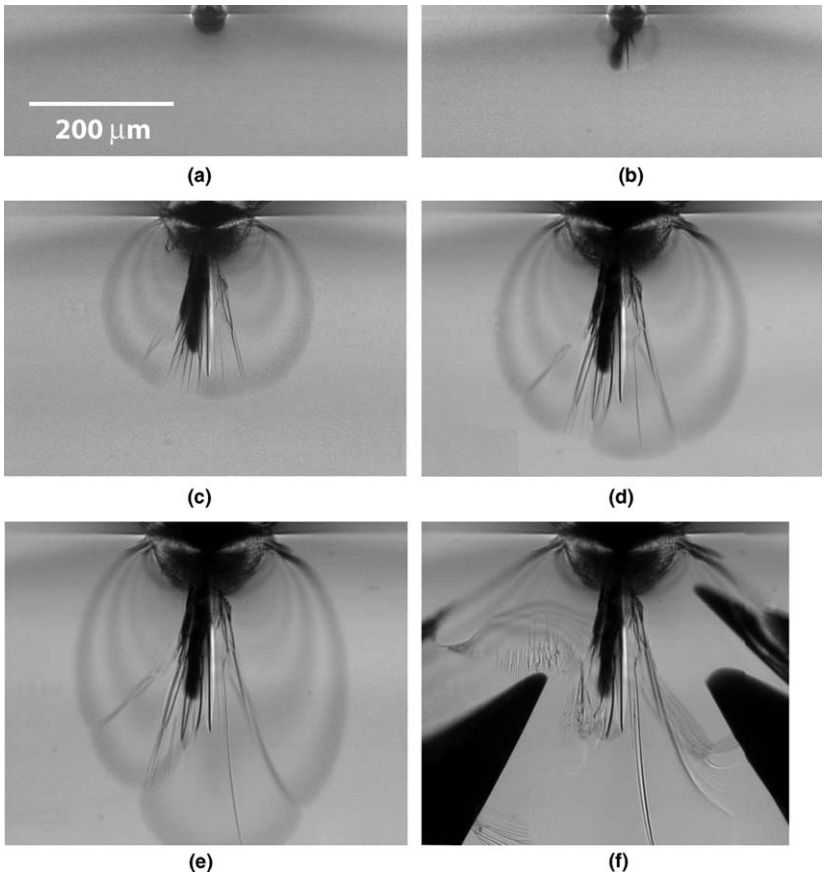

Figure 1. Side view sequence showing median crack evolution in soda-lime glass plate of thickness $d = 1.5$ mm on polycarbonate substrate subjected to Vickers indentation: (a) $P = 30$ N, (b) $P = 38$ N, (c) $P = 175$ N, (d) $P = 272$ N, (e) $P = 307$ N, (f) $P = 308$ N. Note median crack initiation in (b) and ensuing plate failure in (f).

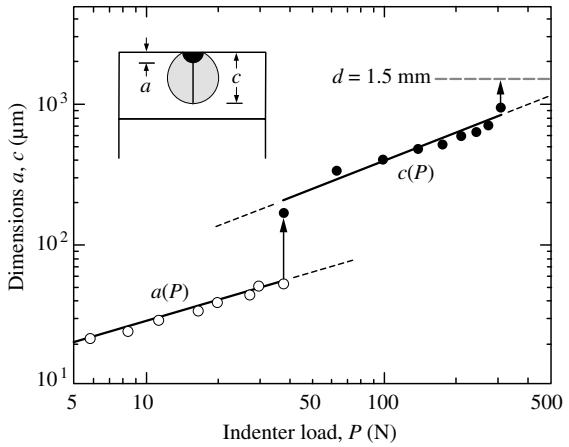

Figure 2. Plot of Vickers plastic zone depth a (unfilled symbols) and median crack depth c (filled symbols) as function of load P for glass thickness $d = 1.5$ mm. Symbols are experimental data, lines are analytical fits, arrows indicate instabilities.

strictly pertain to monoliths, they appear to describe the bilayer data in Figure 2 relatively well up to failure. (In this context, note that the fitted value of K_c/χ compares with 11.9 MPa $m^{1/2}$ from an earlier study of median crack depth in monolithic soda-lime glass [14].) This confirms that the influence of superimposed flexure is not felt strongly until the load is high and the cracks enter the lower half of the plate.

To emphasize this last point, Figure 3 shows a plot of the quasiplastic zone depth a_I (unfilled symbols) at crack initiation and median crack depth c_F (filled symbols) at failure for several bonded glass plates as a function of glass thickness d. The mean dimension $a_I = 50\ \mu m =$ constant (horizontal line) fits the $a_I(d)$ data over the data range, within the scatter, suggesting that initiation events within the small quasiplastic zone are relatively insensitive to thickness effects. The wide scatter in this particular data set reflects the stochastical nature of microcrack flaw generation within the quasiplastic zone. The dimension c_F is much more sensitive to d, and can be adequately represented by the simple proportionality relation $c_F \approx 0.5d$ over the data range (inclined line). The threshold condition for median crack initiation, exemplified by the crossover in the two lines, is apparent in this plot [25].

Figure 4 is a corresponding plot of critical loads P_I for median crack initiation (unfilled symbols) and P_F for ensuing failure (filled symbols), as functions of plate thicknesses d. Again, there is a relatively wide scatter in the initiation condition, somewhat less in the failure condition. The mean value $P_I \approx 30$ N (horizontal line) fits the $P_I(d)$ initiation data over the experimental range,

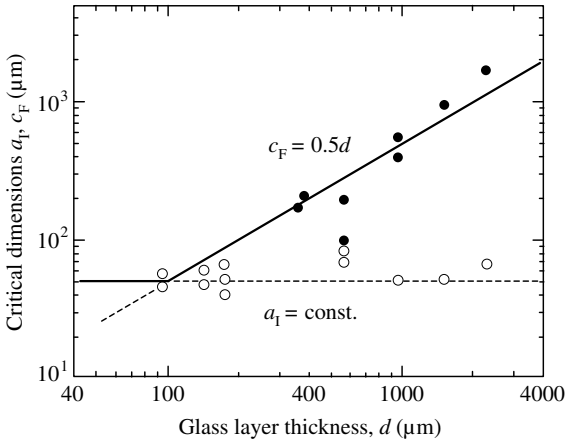

Figure 3. Plot of critical quasiplastic zone depth a_I (unfilled symbols) at initiation and median crack depth c_F (filled symbols) at failure as function of plate thickness d, for Vickers indentations on glass plates bonded to polycarbonate base.

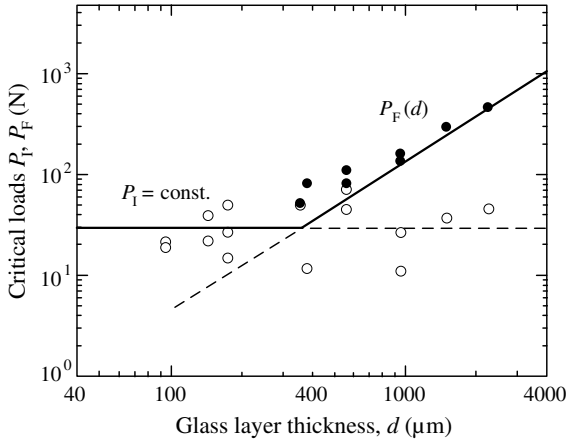

Figure 4. Plot of critical loads P_I for median crack initiation (unfilled symbols) and P_F for ensuing failure (filled symbols), as functions of plate thicknesses d, for Vickers indentations on glass plates bonded to polycarbonate base.

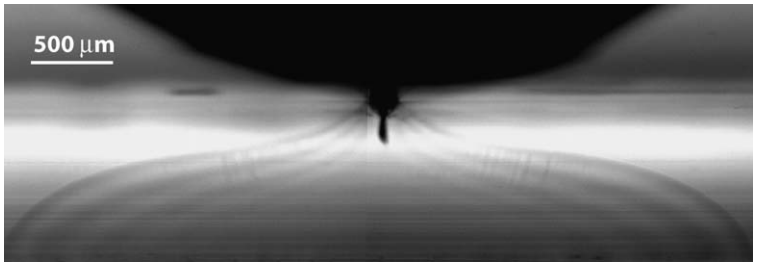

Figure 5. Side view showing failure in soda-lime glass plate of thickness $d = 1$ mm on polycarbonate substrate subjected to Vickers indentation at $P = 90$ N, for specimen with glass undersurface preabraded with SiC grit. An upward-extending radial crack near-orthogonal to the viewing axis has initiated at bottom surface and merged with downward extending median crack. Only glass layer and Vickers indenter (out of focus) are shown.

within the scatter, independent of d. The $P_F(d)$ failure data follow the relation $P_F/d^{3/2} = K_c/2^{3/2}\chi$ (inclined line), obtained by substituting $c_F = d/2$ into Eq. (1b). For plates of thickness $d > 300$ μm approximately, failure occurs directly from stably propagating median cracks. For $d < 300$ μm, failure occurs spontaneously from the quasiplastic zones, without any stable crack growth phase [26]. Note the higher loads required to take the median cracks to failure at larger d in the post-threshold region.

Figure 5 shows a special case in which a glass plate of thickness $d = 1$ mm was preabraded at its undersurface prior to bonding to the polycarbonate base. In this case median cracks initiated first and began to spread downward, in a similar manner to Figure 1. At $P = 90$ N a radial crack initiated from the lower crack surface and spread outward and upward, merging with a downward extending near-coplanar median crack. In this case median–radial crack interaction is pronounced, highlighting the complexity of failure when more than one mode is present.

The present study has described median crack evolution in a model bilayer system consisting of a glass plate bonded to a polycarbonate base, with a Vickers pyramid as indenter. These results are expected to be quite general for any kind of brittle coating subjected to sharp contacts. At sufficiently large coating thickness, the median crack initiates and grows stably downward toward the plate mid-plane, at which point it becomes dominated by flexure-induced tensile stresses and accelerates through the coating. Corresponding critical failure loads diminish with decreasing layer thickness. At small coating thicknesses, crack instability coincides with initiation, so failure can be spontaneous. Thus the median failure mode can be highly deleterious in brittle layer systems.

Some limitations in the current analysis should be acknowledged. We have considered only monotonic loading during the crack evolution from initiation to failure. At no point in our experiments was the indenter unloaded and reloaded. It is well documented that the median cracks can expand in size on unloading, as the constraining elastic component of the indentation field is removed [27–29]. However, this expansion is predominantly in the lateral direction, not downward, so the depths measured here may be considered representative of median cracks in general. It is implicit in Eqs. (1a) and (1b) that H and K_c are size-invariant, a reasonable approximation for homogenous brittle materials like the silicate glass used here but subject to some departures for polycrystalline ceramics. Effects of slow crack growth have not been considered—it is well known that median/radial cracks can grow steadily with time in moist environments, even after completion of the indentation cycle [30]. Fatigue effects are much more profound in multi-cyclic loading, where the quasiplastic zone can expand dramatically by a mechanical fatigue mechanism, greatly expanding the median cracks in all dimensions [31], even with blunt indenters [32]. Nevertheless, the current results suffice to highlight the intrinsic instability in the median crack mode in thin plates on compliant supports.

This work was supported by a grant from the US National Institute of Dental and Craniofacial Research (PO1 DE10976).

[1] D.B. Marshall, Am. Ceram. Soc. Bull. 71 (1992) 969.
[2] M.C. Shaw, D.B. Marshall, M.S. Dadkhah, A.G. Evans, Acta Metall. 41 (1993) 3311.
[3] L. An, H.M. Chan, N.P. Padture, B.R. Lawn, J. Mater. Res. 11 (1996) 204.
[4] H. Liu, B.R. Lawn, S.M. Hsu, J. Am. Ceram. Soc. 79 (1996) 1009.
[5] H.M. Chan, Annu. Rev. Mater. Sci. 27 (1997) 249.
[6] T.J. Lardner, J.E. Ritter, G.-Q. Zhu, J. Am. Ceram. Soc. 80 (1997) 1851.
[7] Y.G. Jung, S. Wuttiphan, I.M. Peterson, B.R. Lawn, J. Dent. Res. 78 (1999) 887.
[8] B.R. Lawn, Y. Deng, P. Miranda, A. Pajares, H. Chai, D.K. Kim, J. Mater. Res. 17 (2002) 3019.
[9] S. Wuttiphan, B.R. Lawn, N.P. Padture, J. Am. Ceram. Soc. 79 (1996) 634.
[10] R. Lakshminarayanan, D.K. Shetty, R.A. Cutler, J. Am. Ceram. Soc. 79 (1996) 79.
[11] J.R. Kelly, J. Prosthet. Dent. 81 (1999) 652.
[12] H. Chai, B.R. Lawn, S. Wuttiphan, J. Mater. Res. 14 (1999) 3805.
[13] B.R. Lawn, Y. Deng, V.P. Thompson, J. Prosthet. Dent. 86 (2001) 495.
[14] B.R. Lawn, E.R. Fuller, J. Mater. Sci. 10 (1975) 2016.
[15] Y.-W. Rhee, H.-W. Kim, Y. Deng, B.R. Lawn, J. Am. Ceram. Soc. 84 (2001) 561.
[16] B.R. Lawn, T.R. Wilshaw, J. Mater. Sci. 10 (1975) 1049.
[17] J.T. Hagan, M.V. Swain, J. Phys.: D 11 (1978) 2091.
[18] J.T. Hagan, J. Mater. Sci. 14 (1979) 2975.
[19] B.R. Lawn, N.P. Padture, H. Cai, F. Guiberteau, Science 263 (1994) 1114.
[20] Y. Zhang, S. Bhowmick, B.R. Lawn, J. Mater. Res. 20 (2005) 2021.
[21] Y. Zhang, B.R. Lawn, J. Biomed. Mater. Res. 69B (2004) 166.
[22] S. Bhowmick, Y. Zhang, B.R. Lawn, J. Mater. Res. 20 (2005) 2792.
[23] B.R. Lawn, M.V. Swain, J. Mater. Sci. 10 (1975) 113.
[24] Y.-G. Jung, A. Pajares, R. Banerjee, B.R. Lawn, Acta Mater. 52 (2004) 3459.
[25] B.R. Lawn, D.B. Marshall, J. Am. Ceram. Soc. 62 (1979) 347.
[26] T.P. Dabbs, C.J. Fairbanks, B.R. Lawn, In: S.W. Freiman, C.M. Hudson (Eds.), Methods for Assessing the Structural Reliability of Brittle Materials. ASTM Special Technical Publication 844, Philadelphia, PA: ASTM, 1984, pp. 142.
[27] D.B. Marshall, B.R. Lawn, J. Mater. Sci. 14 (1979) 2001.
[28] B.R. Lawn, A.G. Evans, D.B. Marshall, J. Am. Ceram. Soc. 63 (1980) 574.
[29] R.F. Cook, G.M. Pharr, J. Am. Ceram. Soc. 73 (1990) 787.
[30] B.R. Lawn, K. Jakus, A.C. Gonzalez, J. Am. Ceram. Soc. 68 (1985) 25.
[31] F. Guiu, M. Reece, D.A.J. Vaughan, J. Mater. Sci. 26 (1991) 3275.
[32] D.K. Kim, Y.-.G. Jung, I.M. Peterson, B.R. Lawn, Acta Mater. 47 (1999) 4711.